

Comparison of Formation Conditions of Source Rocks of Fengcheng and Lucaogou Formations in the Junggar Basin, NW China: Implications for Organic Matter Enrichment and Hydrocarbon Potential

Shiju Liu^{1, 2, 3}, Gang Gao^{1, 2}, Wenzhe Gang^{1, 2}, Baoli Xiang⁴, Ming Wang⁴, Chengyun Wang⁵



1. College of Geosciences, China University of Petroleum, No. 18 Fuxue Road, Beijing 102249, China

2. State Key Laboratory of Petroleum Resource and Prospecting, China University of Petroleum, No. 18 Fuxue Road, Beijing 102249, China

3. PetroChina Research Institute of Petroleum Exploration & Development, Beijing 100083, China

4. Experimental Testing Institute, PetroChina Xinjiang Oilfield Company, Karamay 834000, China

5. Exploration and Development Research Institute of PetroChina Huabei Oilfield Company, Renqiu 062552, China

 Shiju Liu: <https://orcid.org/0000-0003-4630-896X>;  Gang Gao: <https://orcid.org/0000-0002-7967-9225>

ABSTRACT: Shales in the Carboniferous–Permian Fengcheng (FC) and Lucaogou (LCG) formations in Junggar Basin are important organic rich rocks containing significant oil resources. To evaluate the difference in sedimentary environment conditions and hydrocarbon-generating potential between the FC and LCG formations. Total organic carbon (TOC), Rock-Eval pyrolysis, solvent extraction, column fractionation, stable carbon isotope, gas chromatography-mass spectrometry (GC-MS) of saturated hydrocarbons and organic petrology from the source rocks of FC and LCG formations. were analyzed. The biomarker composition indicates that during the deposition of FC, LCG-1 to LCG-2, the sedimentary environment for the source rock formations changed with gradual decrease of salinity, from anoxic to dyoxic/suboxic in redox conditions, and from strong stratification to weakened stratification of water. The FC Formation source rock, with main telalginite (planktonic green algae), archaeobacteria and minor terrestrial organic matter, deposited in the environment characterized by high salinity and strongly reducing condition. Its TOC content is relatively low with a high original hydrocarbon-generating potential of unit organic material. The LCG Formation source rock deposited in the environment with low salinity and large variations, the organic matter is mainly sourced from telalginite (planktonic green algae), lamalginite, bacteria and higher plants, resulting in strong heterogeneity of the source rock. The abundance of TOC is high, but the original hydrocarbon generation potential of unit organic matter is lower than that of FC Formation. The results provide a geochemical basis for further study of saline-brackish water sedimentary environment shales in the Junggar Basin.

KEY WORDS: geochemistry, biogenic precursors, depositional conditions, Fengcheng Formation, Lucaogou Formation, Junggar Basin.

0 INTRODUCTION

Modern oil and gas exploration is characterized by increasing development of unconventional oil and gas (Liu et al., 2021; Ghanizadeh et al., 2015; Jarvie, 2012, 2010; Che et al., 2010; Liu and Liu, 2005). Unconventional oil and gas are mainly characterized by the integration of source rocks and reservoirs, which forms a “self-generating and self-storing” petroleum system (Liu et al., 2018; Nie et al., 2016; Gao et al.,

2013; Wu et al., 2013; Kuhn et al., 2012; Liang et al., 2012), which are conducive to the efficient accumulation of oil and gas. The enrichment of shale/tight oil and gas is closely related to the sedimentary conditions of source rocks and the source of organic matter (Gao et al., 2018; Liu et al., 2017; Zou et al., 2013, 2011). It is important to analyze the evolution of the sedimentary conditions of source rocks and to compare the mechanisms of organic matter enrichment to better understand the accumulation and distribution of shale/tight oil and gas. Some researchers have reported that many lacustrine high-quality source rocks are related to the mixed fine-grained deposition conditions in lacustrine basins with specific but varying degrees of salinity (Jin et al., 2008; Zhu et al., 2004). The Carboniferous–Permian Fengcheng Formation (FC Fm) and Lucaogou Formation (LCG Fm) in the Junggar Basin, North-

*Corresponding author: gaogang2819@sina.com

© China University of Geosciences (Wuhan) and Springer-Verlag GmbH Germany, Part of Springer Nature 2023

Manuscript received April 30, 2021.

Manuscript accepted July 9, 2021.

Liu Shiju, Gao Gang, Gang Wenzhe, Xiang Baoli, Wang Ming, Wang Chengyun, 2023. Comparison of Formation Conditions of Source Rocks of Fengcheng and Lucaogou Formations in the Junggar Basin, NW China: Implications for Organic Matter Enrichment and Hydrocarbon Potential. *Journal of Earth Science*, 34(4): 1026–1040. <https://doi.org/10.1007/s12583-021-1566-0>. <http://en.earth-science.net>

west China are typical fine-grained deposits in saline lacustrine facies (Gao et al., 2018; Wang et al., 2018; Qu et al., 2017; Ren et al., 2017). Although the FC and the LCG Fms were deposited in different periods, the compositions of the biomarkers in the source rocks are similar and inherited to some extent. In this study, the sedimentary environment and biological sources of the FC Fm and LCG Fm in the Junggar Basin were systematically analyzed. A comprehensive study on the evolution of the sedimentary conditions of organic matter enrichment in the source rocks of the brackish lacustrine basin is helpful in determining the favorable sedimentary conditions for the development of source rocks in other areas. Therefore, it helps in predicting effective source rocks and improves the understanding of the conditions for the accumulation of shale oil and gas resources or for the enrichment of organic matter in the source rock.

1 GEOLOGICAL SETTING

The Junggar Basin is located in the northern part of the Xinjiang Uygur Autonomous Region of China. It is bounded by the Harat and Delun Mountains in the northwest and the Qingge Lidi Mountains in the northeast. The Junggar Basin is adjacent to Mount Krameli (east), Mount Chai (west), Mount Irinhebirgen (southwest), and Mount Bogda (southeast) (Wang et al., 2000) (Fig. 1), and has experienced many tectonic movement cycles, such as the Hercynian, Indo-China, Yanshan, and Himalayan, resulting in the formation of a large superimposed basin (Zhang and Zhang, 2006). The subsidence of the pre-Carboniferous basement in the basin is relatively large, and the sedimentary rocks in the central depression have a thickness of 13–16 km (Chen et al., 2007; Zhang et al., 2006; Kuang et al., 1999).

The FC Fm, which is mainly distributed in the Mahu sag of a secondary tectonic unit of the Junggar Basin, extends westward to the Wuxia and Kebai fault zones. The southern area of the Mahu sag is connected to the Zhongguai uplift and the Dabasong uplift and is adjacent to the Xiayan uplift, Yingxi depression, and the Quartz Tan uplift in the east, with a total area of ~5 200 km² (Fig. 1a). A series of strata successively developed in the Mahu sag during the Carboniferous, Permian, Triassic, Jurassic, Cretaceous, Tertiary, and Quaternary periods. Most of the strata are in unconformable contact (Fig. 1b) in which reservoir-caprock assemblages developed on each horizon, consisting of multiple assemblages of varying qualities. The major source rocks occur in the FC Fm in the Mahu sag, with some of them in the Middle Permian Lower Wuerhe Fm and Middle Carboniferous Jiamuhe Fm (Cao et al., 2020) (Fig. 1b). The FC Fm was buried at a depth of 2 600–6 500 m and was 150–1 000 m thick on average, with the thickest point reaching 1 800 m. It is in unconformable contact with the Lower Jiamuhe Fm and Upper Xiazijie Fm (Lu et al., 2012).

The Jimusaer sag, located in the eastern Junggar Basin, is a subsag developed on the eastern uplift of the first-order structural unit and bounded by thrust faults on its southern, western, and northern boundaries (Fig. 1). It is surrounded by the Bogeda Mountain tectonic belt through the Santai fault in the south and separated by the Xidi fault in the west and the Jimusaer fault and Shaiqi uplift in the north; it transitions to the west Gu-cheng uplift in the east. On a 2D plane, the Jimusaer sag takes

on the shape of an irregular polygon, covering an area of ~1 278 km² (Zhang et al., 2003). Currently, it has a dustpan-like structure with a fault in the west and an overlap in the east. The LCG Fm and Jingjingzigou Fm are in conformable contact, with the thickest part located in the central depression (Fig. 1d). The thickness averages 100–320 m, which decreases towards the edges and is divided into two longitudinal sections. The formations consist mainly of a set of shale, thin-layered sandy dolomite, and dolomitic siltstone, which primarily generate hydrocarbons in the sag (Guo and Li, 2009; Liu et al., 2006; Shi et al., 2005). Currently, crude oil found in the LCG Fm and Wutonggou Fm is sourced from this set of source rocks (Gao et al., 2016; Jiang et al., 2015; Kuang et al., 2013, 2012; Sun, 2012).

2 SAMPLING AND METHODS

2.1 Samples

In order to conduct experimental analysis on the source rock of the LCG Fm in the Jimusaer sag, 152 shale core samples were obtained from drilling wells shown in Fig. 1c. Among them, 83 samples were collected from the upper part of the Lucaogou Fm (LCG-2), with 69 samples collected from the lower part (LCG-1). In FC Fm, a total of 135 shale core samples were obtained from nine wells in the Mahu sag (Fig. 1a). Some geochemical experiments were conducted to clarify the mudstone characteristics in the three horizons from the 287 collected samples.

2.2 TOC and Rock-Eval

Before the start of the experiments, the samples were screened with an 80-mesh sieve. For meeting the requirements of the analytical instrument and for the convenience of subsequent experiments, all shale samples were crushed into powder smaller than 80-mesh size prior to conducting the experiments. The TOC and rock pyrolysis was carried out according to Chinese Industry Standard GB/T 19145-2003 and GB/T 18602-2012, respectively. Those described by Li et al. (2019a, b, 2017). A Leco CS-230 Carbon analyzer was used for the TOC (total organic carbon) analysis. Free hydrocarbon content (S_1 ; mg HC/g rock), pyrolyzed hydrocarbon (S_2 ; mg HC/g rock) and maximum pyrolysis yield (T_{max}) (the temperature of maximum pyrolysis yield in °C) data were obtained by Rock-Eval analysis.

2.3 Gas Chromatograph-Mass Spectrometer and Stable Carbon Isotope Measurements

Extraction and fractionation of soluble organic matter in source rocks and GC-MS analysis of saturated hydrocarbons are consistent with those described by Gao et al. (2018). The carbon isotope analyses of the extracts are consistent with those described by Luo et al. (2018).

2.4 Petrographic Analysis

Organic petrological characteristics were described by using a Leica MPV microscope equipped with a 50× and 20× objective and oil immersion under reflected and blue fluorescent light. The polished thin sections for microscopic observation were prepared perpendicular to the bedding planes.

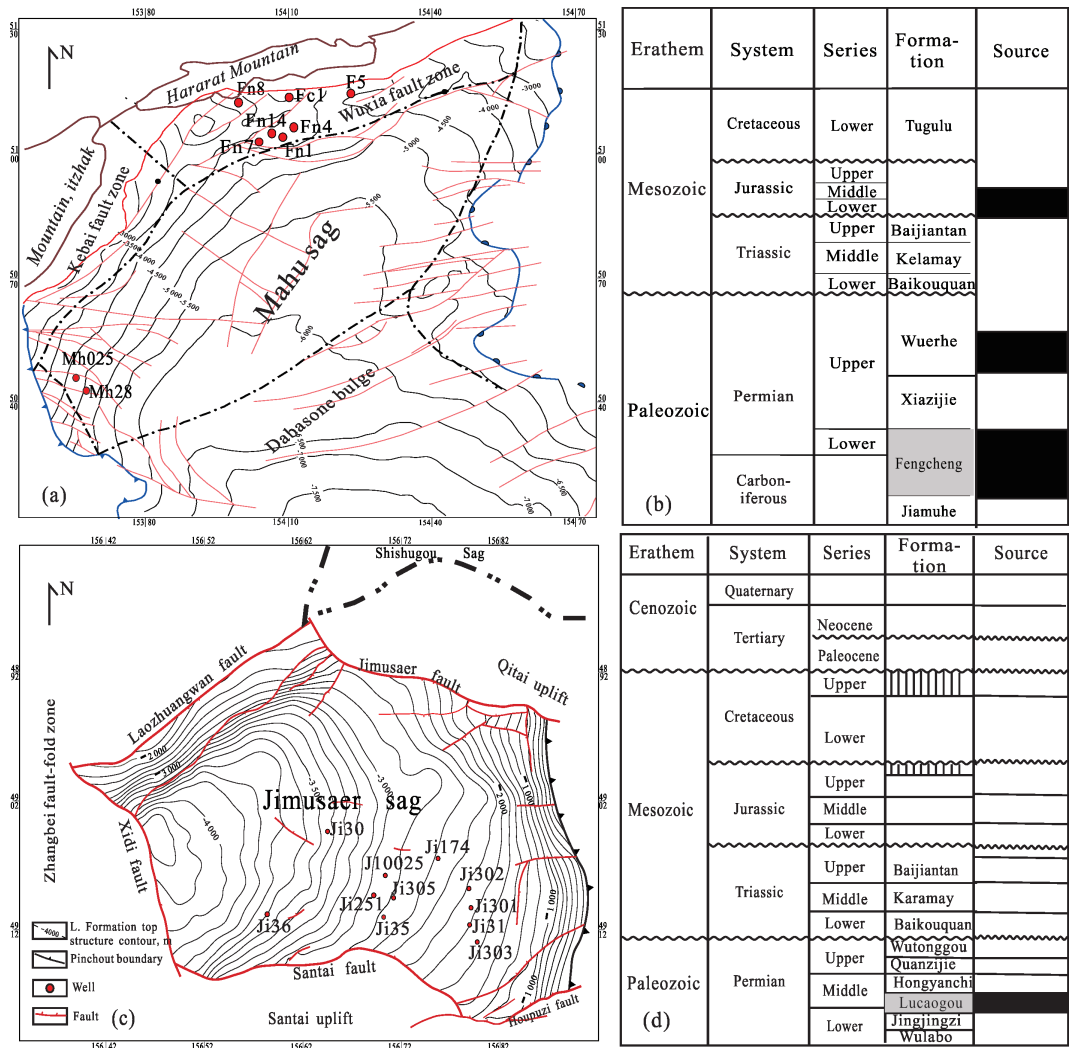


Figure 1. Locality and Stratigraphic column of the Mahu and Jimusaer sag in Junggar Basin. (a) Locality of Mahu sag; (b) stratigraphic column of Mahu sag; (c) locality of Jimusaer sag; (d) stratigraphic column of Jimusaer sag.

3 RESULTS

3.1 Source Rock Characteristics

The FC Fm, LCG-1, and LCG-2 shales in the Mahu and Jimusaer sags contain variable TOC contents in the range of 0.36 wt.%–4.43 wt.% (ave = 1.06 wt.%), 0.36 wt.%–10.3 wt.% (ave = 4.06 wt.%), and 0.24 wt.%–30.10 wt.% (ave = 5.67 wt.%), respectively (Table S1 and Table 1). The S_1 values were 0–4.70 mg HC/g rock (ave = 0.73 mg HC/g rock), 0.02–8.89 mg HC/g rock (ave = 1.12 mg HC/g rock), and 0.01–4.31 mg HC/g rock (ave = 0.91 mg HC/g rock) for the FC Fm, LCG-1, and LCG-2 shales, respectively (Table S1 and Table 1). The S_2 values were 0.25–59.47 mg HC/g rock (ave = 4.47 mg HC/g rock), 0.17–75.89 mg HC/g rock (ave = 20.95 mg HC/g rock), and 0.25–202.56 mg HC/g rock (ave = 37.29 mg HC/g rock) for the FC Fm, LCG-1, and LCG-2 shales, respectively (Table S1 and Table 1). The TOC and $S_1 + S_2$ values suggested that these sediments were mostly good-to-excellent source rocks (Fig. 2). In Fig. 2, the TOC values of the FC, LCG-1, and LCG-2 Fm shales are strongly positively correlated with $S_1 + S_2$, whereas the FC Fm shales displayed higher $S_1 + S_2$ values than the LCG shales do for the same TOC content.

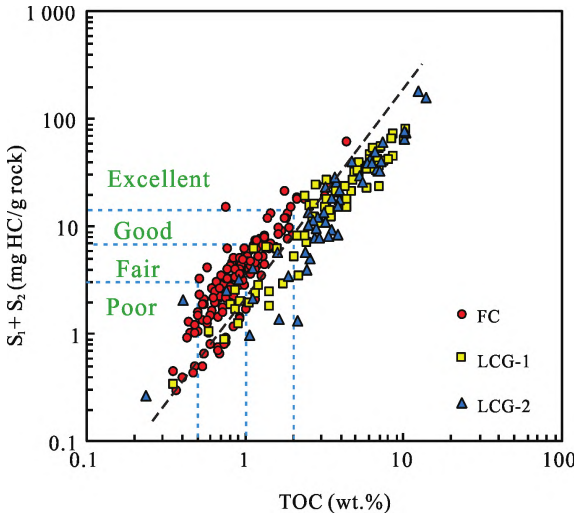


Figure 2. Plot of TOC versus $S_1 + S_2$, showing potential hydrocarbon generative (after Waples, 1985).

The HI values in the FC, LCG-1, and LCG-2 shales had a wider distribution, ranging from 68–1 872 mg HC/g TOC

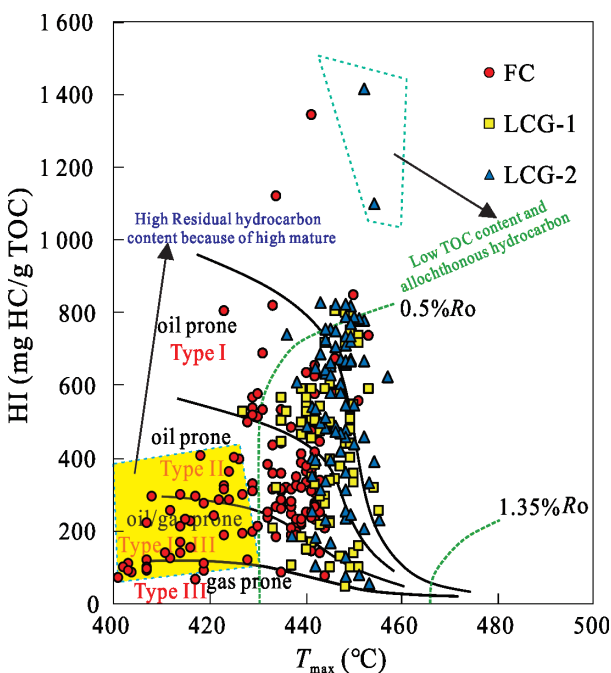


Figure 3. HI versus T_{max} diagram based on rock pyrolysis of whole rock (after Mukhopadhyay et al., 1995).

(ave = 346 mg HC/g TOC), 47–806 mg HC/g TOC (ave = 427 mg HC/g TOC), and 56–1 417 mg HC/g TOC (ave = 540 mg HC/g TOC), respectively. The T_{max} of the FC Fm shales was extremely low, falling into the range of 412–451 °C (ave = 434 °C) (Table S1); this is due to the high residual hydrocarbon content. As illustrated in Fig. 3, the FC, LCG-1, and LCG-2 shales were dominated by Type I–II kerogen, which agreed with the high HI values.

3.2 Aliphatic Hydrocarbons

The total ion current (TIC), terpane m/z 191 and Sterane m/z 217 of gas chromatography-mass spectrometer (GC-MS) of saturated fraction are shown in Fig. 4. In the TIC spectrum, the n-alkane distribution showed a unimodal distribution pattern with a maximum peak at C_{25} or C_{27} for the LCG-1 and LCG-2 shales. However, the major peak carbon types of the FC Fm mudstone were C_{22} and C_{24} (Fig. 4). Most samples contained a high abundance of β -carotane, as illustrated in Fig. 4. The $C_{30}\alpha\beta$ hopane predominated in the hopane homologues, with a minor of C_{29} $\alpha\beta$ hopane, Ts, Tm, and homohopanes (Fig. 4). The distributions of sterane and diasterane detected in the $m/z = 217$ spectrum, with high abundance of C_{28} and C_{29} regular sterane (Fig. 4). Parameters of saturated hydrocarbons, terpanes and steranes are shown in Table S2, and Table 2, respectively.

Table 1 Statistical data of the tested TOC, Rock-Eval parameters and EOM for the FC Fm, LCG-1 and LCG-2 samples

Index	FC				LCG-1				LCG-2			
	Max	Min	Ave	Num	Max	Min	Ave	Num	Max	Min	Ave	Num
TOC (wt.%)	4.43	0.36	1.06	135	10.30	0.36	4.06	69	30.10	0.24	5.67	83
T_{max} (°C)	455	401	431	135	455	427	444	69	457	436	447	83
S_1 (mg HC/g rock)	4.7	0.00	0.73	135	8.89	0.02	1.12	69	4.31	0.01	0.91	83
S_2 (mg HC/g rock)	59.47	0.25	4.47	135	75.89	0.17	20.95	69	202.56	0.25	37.29	83
HI (mg HC/g TOC)	1872	68	343	135	806	47	427	69	1417	56	540	83
$S_1 + S_2$ (mg HC/g rock)	59.84	0.29	5.20	135	77.28	0.33	22.07	69	204.69	0.26	38.21	83
PI	0.53	0.00	0.16	135	0.49	0.00	0.08	69	0.21	0.00	0.04	83

$HI = S_2/TOC$; $PI = S_1/(S_1 + S_2)$; $HCI = S_1/TOC$.

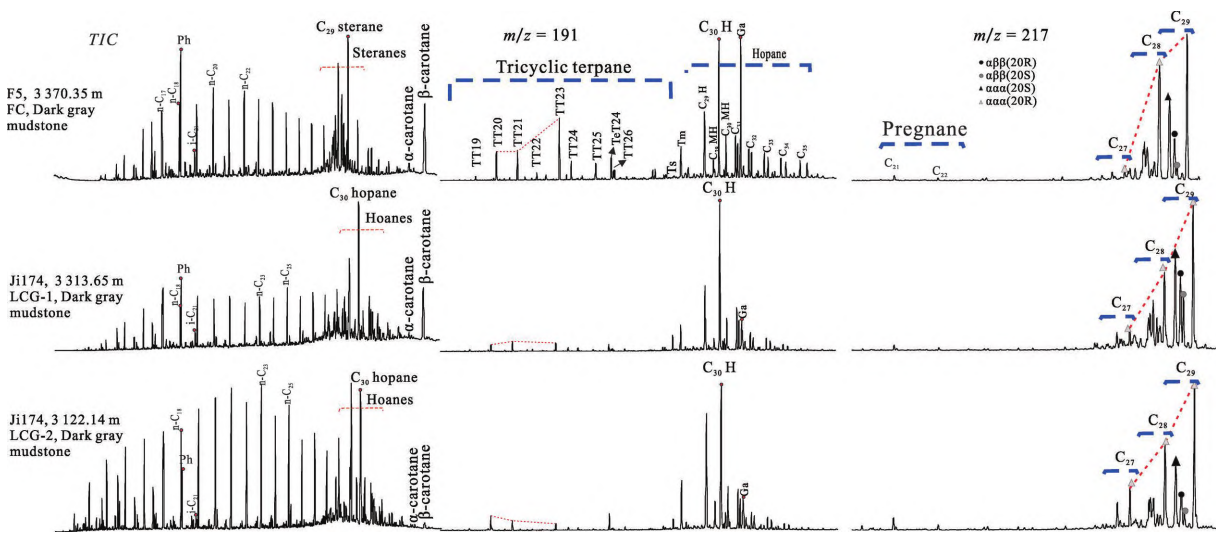


Figure 4. Mass chromatograms of FC Fm, LCG-1 and LCG-2 black shales.

Table 2 Statistical data of the $\delta^{13}\text{C}_{\text{EOM}}$ and aliphatic hydrocarbon parameters of the FC, LCG-1 and LCG-2 samples

Index	FC				LCG-1				LCG-2			
	Max	Min	Ave	Num	Max	Min	Ave	Num	Max	Min	Ave	Num
$\delta^{13}\text{C}_{\text{EOM}}$ (‰)	-28.10	-33.57	-30.25	62	-29.31	-32.97	-30.42	69	-29.16	-34.03	-32.18	83
β -carotane/n- C_{max}	13.14	0.00	1.96	62	3.21	0.00	0.67	69	3.72	0.00	0.30	83
Pr/Ph	1.85	0.34	0.75	62	2.18	0.67	1.14	69	2.30	0.50	1.25	83
Pr/n- C_{17}	2.65	0.34	1.39	62	2.03	0.29	1.12	69	2.67	0.14	0.79	83
Ph/n- C_{18}	6.04	0.37	2.05	62	2.89	0.19	1.31	69	2.43	0.07	0.62	83
OEP	1.22	0.88	1.08	62	1.66	0.97	1.18	69	1.59	0.92	1.22	83
CPI	1.16	0.82	1.04	62	1.54	1.03	1.18	69	1.57	0.91	1.22	83
n- C_{21} /n- C_{22+}	3.47	0.20	1.07	62	2.65	0.34	1.11	69	1.91	0.03	0.83	83
i- C_{19} /n- C_{21}	1.34	0.07	0.52	62	0.37	0.04	0.19	69	0.36	0.01	0.09	83
Gammacerane/ C_{30} $\alpha\beta$ hopane	2.58	0.07	0.57	62	0.31	0.10	0.19	69	0.38	0.05	0.16	83
hopanes/steranes	4.52	0.08	0.48	62	11.69	1.26	4.88	69	13.88	1.71	5.30	83
$\text{C}_{27}/\text{C}_{29}$ $\alpha\alpha\alpha$ 20R sterane	1.01	0.05	0.21	62	0.63	0.13	0.25	69	1.09	0.22	0.51	83
$\text{C}_{28}/\text{C}_{29}$ $\alpha\alpha\alpha$ 20R sterane	1.15	0.48	0.70	62	1.16	0.33	0.65	69	2.91	0.46	0.91	83
$\text{C}_{20}\text{TT}/\text{C}_{23}\text{TT}$	1.65	0.34	0.74	62	2.07	0.58	1.31	69	3.14	0.56	1.47	83
$\text{C}_{22}/\text{C}_{21}\text{TT}$	0.24	0.14	0.20	62	0.32	0.12	0.15	69	0.28	0.05	0.12	83
$\text{C}_{29}\alpha\alpha\alpha$ 20S/(20S + 20R) sterane	0.48	0.23	0.42	62	0.48	0.38	0.44	69	0.48	0.16	0.37	83
$\text{C}_{29}\alpha\beta\beta/(\alpha\beta\beta + \alpha\alpha\alpha)$ sterane	0.60	0.21	0.42	62	0.50	0.25	0.32	69	0.40	0.15	0.22	83
C_{31} 22S/(22S + 22R) homohopane	0.59	0.37	0.55	62	0.60	0.50	0.58	69	0.66	0.53	0.58	83
C_{32} 22S/(22S + 22R) bishomohopane	0.63	0.49	0.58	62	0.60	0.55	0.58	69	0.60	0.47	0.55	83
$\text{C}_{29}\alpha\beta/(\alpha\beta + \beta\alpha)$ hopane	0.91	0.81	0.88	62	0.92	0.84	0.89	69	0.92	0.74	0.85	83
$\text{C}_{30}\alpha\beta/(\alpha\beta + \beta\alpha)$ hopane	0.88	0.65	0.82	62	0.87	0.70	0.80	69	0.89	0.67	0.80	83

CPI. Carbon preference index of n-alkane = $[(\text{C}_{25} + \text{C}_{27} + \text{C}_{29} + \text{C}_{31} + \text{C}_{33})/(\text{C}_{24} + \text{C}_{26} + \text{C}_{28} + \text{C}_{30} + \text{C}_{32}) + (\text{C}_{25} + \text{C}_{27} + \text{C}_{29} + \text{C}_{31} + \text{C}_{33})/(\text{C}_{26} + \text{C}_{28} + \text{C}_{30} + \text{C}_{32} + \text{C}_{34})]/2$ (after Bray and Evans, 1961); OEP. odd-even predominance of n-alkane = $(\text{C}_{23} + 6 \times \text{C}_{25} + \text{C}_{27})/(4 \times \text{C}_{24} + 4 \times \text{C}_{26})$ (after Scanlan and Smith, 1970).

3.3 Organic Petrology Characteristic

It is displayed from organic petrology that the mudstones in the FC Fm and LCG Fm are dominated by sapropel (including algae A recognized as planktonic green algae by Xia et al. (2021) and algae B (lamalginite)) (Figs. 5 and 6). The parental material of FC Fm mudstone is primarily algae A (Figs. 5a, 5c and 5e), and a large amount of framboidal pyrite in the rocks (Figs. 5b, 5d and 5f). The algae A can be identified by the characteristics of high hydrogen concentration (Hackley et al., 2016; Kates, 1977), low reflectance and weak brownish fluorescence. And the pyrite is evidently distinguishable for its high luminescence under white light. The organic matter of source rocks of the LCG Fm contains mainly algae A (green algae), algae B, and a mixture of vitrinite and inertinite (Fig. 6). The lamalginite is mainly distributed parallel to bedding and displays strong yellow fluorescence (Figs. 6a, 6e and 6g).

4 DISCUSSION

4.1 Thermal Maturity

Maturity, one of the key geochemical parameters in evaluating the hydrocarbon potential of source rocks, can frequently be calibrated by using parameters such as the vitrinite reflectance, T_{max} , and production index (PI) (Cheng, 1994; Huang et al., 1984; Tissot and Welte, 1984). The PI values of shale samples showed an increasing trend in the shales: from 0 to 0.53 (ave = 0.16) in FC Fm, from 0 to 0.49 (ave = 0.08) in LCG-1,

and from 0 to 0.21 (ave = 0.04) in LCG-2 (Table S1 and Table 1). In the crossplot of PI ($S_1/(S_1 + S_2)$) versus T_{max} , most of the data points of the shale samples from LCG-1 and LCG-2 were in the oil window with few points in the early oil zone (Fig. 7). However, the FC Fm sample showed a higher PI and a lower T_{max} (Fig. 7). This may be due to the high maturity level and high content of free hydrocarbons in the FC Fm source rock, which is consistent with the higher S_1 value in FC Fm. As the thermal maturity level increases, the HI value decreases. It can be seen from Figs. 8a–8b that the HI values of the LCG Fm do not vary greatly with depth, while the HI of the FC Fm decreases significantly with increasing depth, indicating that the thermal maturity of the FC Fm is higher than that of the LCG Fm.

Miscellaneous maturity indicators can be used to determine the thermal maturity level of organic matter, such as the CPI and OEP, hopanoids C_{31} 22S/(22S + 22R), homohopanes, and other similar indices (Seifert and Moldowan, 1986). The C_{31} 22S/(22S + 22R) homohopane and C_{32} 22S/(22S + 22R) bi-homohopane ratios of the study samples are at their equilibrium values (0.57–0.62) (Fig. 9b) during the thermal maturation of organic matter (Luo et al., 2016; Peters et al., 2005), indicating that the samples studied are almost all staged in the early oil window. In addition, the plot of the $\text{C}_{29}\alpha\beta/(\alpha\beta + \beta\alpha)$ hopane vs. $\text{C}_{30}\alpha\beta/(\alpha\beta + \beta\alpha)$ hopane also showed that the samples studied did not reach equilibrium (0.90–0.95) (Fig. 9a) (Peters et al., 2005, George et al., 2001), indicating low thermal maturity

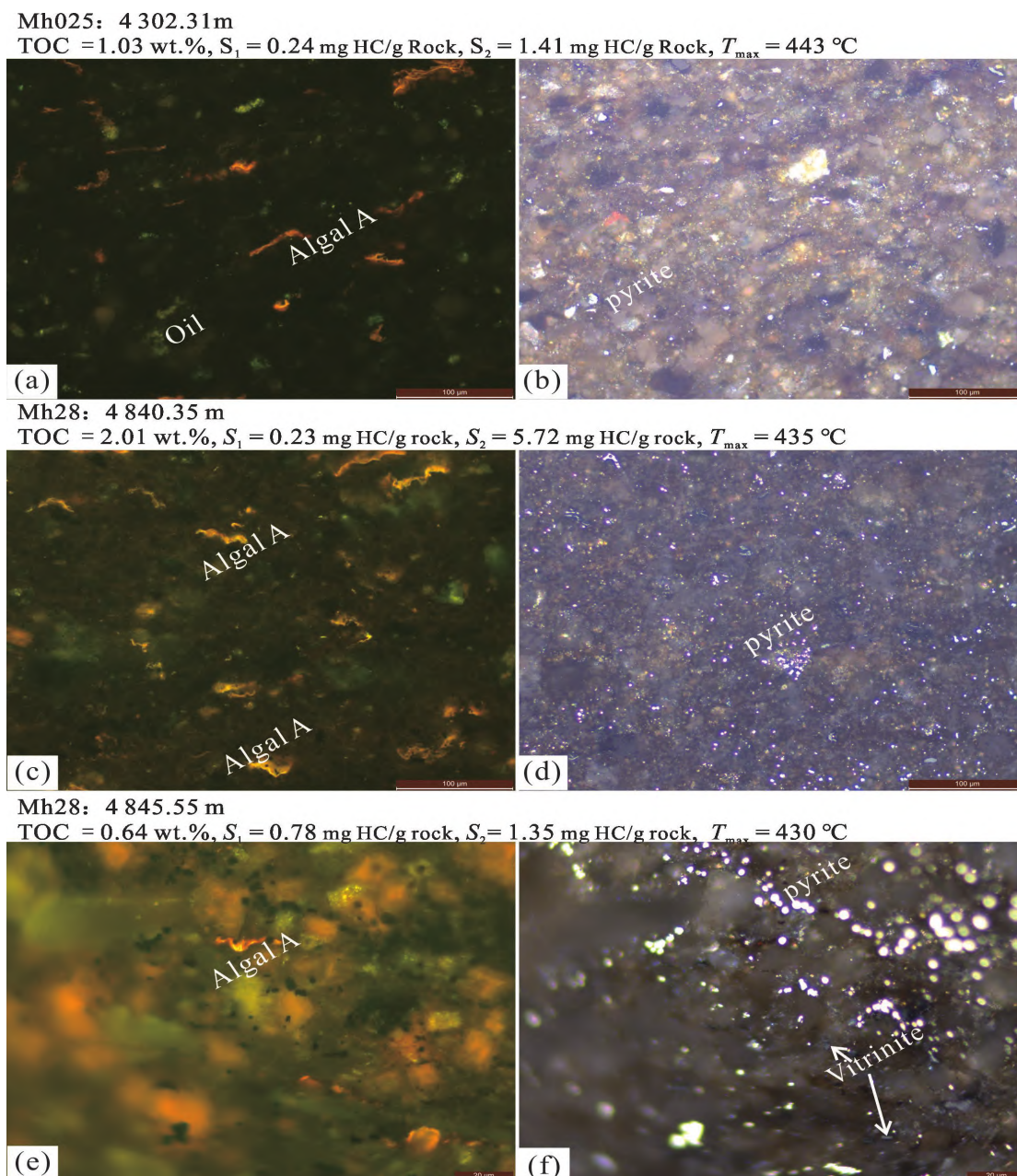


Figure 5. Photomicrographs showing algal A (green algae), oil and pyrite in the FC Fm sediments from the Junggar Basin. (a) Fluorescent light, shale; (b) the same scope as (a) under reflected light; (c) fluorescent light, shale; (d) same field as (c) under reflection light; (e) fluorescent light, shale; (f) same field as (e) under reflected light.

of the samples. The LCG-2 Samples contained extraordinarily low ratios of $C_{29} \alpha\alpha 20S/(20S + 20R)$ and $C_{29} \alpha\beta\beta/(\alpha\beta\beta + \alpha\alpha\alpha)$ sterane (Table S2 and Table 2), both of which were much lower than their equilibrium values, indicating low thermal maturity (Fig. 9c). The values of the $C_{29} \alpha\alpha 20S/(20S + 20R)$ sterane of the LCG-1 and FC Fm samples were not significantly different, but the $C_{29} \alpha\beta\beta/(\alpha\beta\beta + \alpha\alpha\alpha)$ sterane ratios of FC Fm. were larger than those of LCG-1, which indicated that the $C_{29} \alpha\alpha 20S/(20S + 20R)$ sterane ratios of the LCG and FC Fm samples reached the end of the equilibrium range before reaching their equilibrium values, and the FC Fm mudstone samples reached the mature stage. As shown in Fig. 9d, the FC Fm mudstone samples have a higher degree of thermal evolution than LCG-1

and LCG-2 and have reached the mature stage, while the LCG-1 and LCG-2 mudstone samples were in the low-to-medium maturity stage.

The cross plot of saturated hydrocarbons indicates that the shale in the LCG Fm may have reached the early oil-generation window and that in the FC Fm may have reached the peak oil window.

4.2 Biological Sources and Environment Analysis

The study on the biological sources of organic matter can be intuitively conducted by the observation of solid organic matter of source rock samples (Luo et al., 2018). The source of organic matter in source rocks of the FC Fm is mainly plank-

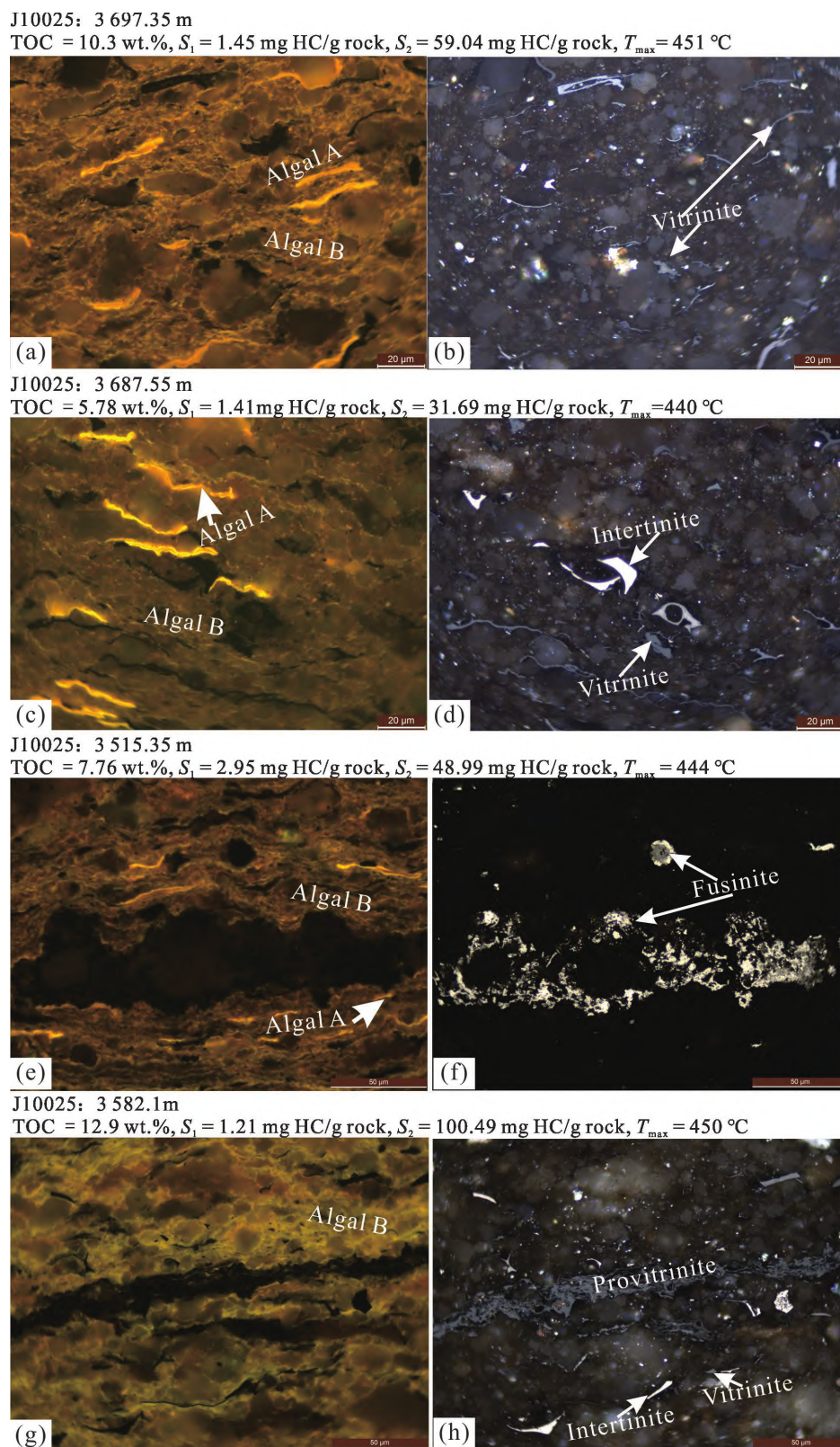


Figure 6. Photomicrographs showing algal A (green algae), algal B (lamalginite), fungus, provitrinite, inertinite and vitrinite in the LCG Fm, sediments from the Junggar Basin. (a) Fluorescent light, shale; (b) same field as (a) under reflected light; (c) fluorescent light, shale; (d) same field as (c) under reflected light; (e) blue fluorescent light, shale; (f) same scope field as (e) under reflected light; (g) blue fluorescent light, shale; (h) same scope field as (g) under reflected light.

tonic algae (algae A) with monotonous species (Figs. 5a, 5c and 5e). The organic matter is mainly sourced from ancient salt-tolerant green algae (*Dunaliella*) (Xia et al., 2021). The in-

put of terrigenous detrital materials is extremely weak, and the pyrite is relatively developed (Figs. 5b, 5d and 5f), which implies that the sedimentary water column of the FC Fm is char-

acterized by high salinity and reducing conditions. The green algae (algae A) can be observed in the LCG Fm (Figs. 6a, 6c and 6f). However, another source of organic matter (algae B), which is similar to lamalginite in the macerals observed in the thin sections of rocks (Liu et al., 2017), was developed in the LCG Fm (Fig. 6). In different LCG Fm samples, there were also evident changes in the relative enrichment of the two algae. For instance, algae B developed significantly in the LCG-2 Member (Fig. 6g). At the same time, the contribution of terrestrial organic matter in the LCG Fm is relatively high, but the content of framboidal pyrite is low (Fig. 6), indicating the freshwater input during the depositional period of the LCG Fm. Comparing the organic petrological characteristics of source rocks from the FC and LCG Fms, the two sets of source rocks have certain inheritance in terms of the source of organic matter. The source of organic matter in the FC Fm is relatively stable and dominated by salt-tolerant algae. While the organic matter in the LCG Fm was characterized by diverse and complex sources, which was consistent with the wide range of HI variation in the LCG Fm.

The carbon isotopes of kerogen are mainly affected by biological sources of organic matter and generally shows heavier carbon isotopes in the oil produced by humic kerogen ($> -26\text{‰}$) than that produced by sapropelic kerogen ($< -28\text{‰}$) (Borjigen et al., 2014). The $\delta^{13}\text{C}_{\text{EOM}}$ values range from -33.57‰ to -28.10‰ (ave = -30.25‰), -32.97‰ to -29.31‰ (ave = -30.42‰), and -34.03‰ to -29.16‰ (ave = -32.18‰) for the FC Fm, LCG-1, and LCG-2 shales, respectively (Table S2 and Table 2). The $\delta^{13}\text{C}_{\text{EOM}} < -28\text{‰}$ in the studied samples revealed that the organic matter was derived primarily from sapropelic organic matter (OM), with a litter contribution from terrigenous OM. This is also consistent with the high HI values. The carbon isotopes of organic matter are also affected by the deposition conditions and the diversity of aquatic algae; the higher the salinity, the higher the organic carbon isotope values (Duan et al., 2003). The presence of β -carotane, which is typically an indicator of an anoxic saline lacustrine environment (Jiang and Flower, 1986; Hall and Douglas, 1981), is highly abundant, as

indicated by the values of β -carotane/ $n\text{-C}_{\text{max}}$ (Luo et al., 2018) (Table S2 and Table 2). The FC, LCG-1, and LCG-2 shales contain variable β -carotane/ $n\text{-C}_{\text{max}}$ ratios, falling in the range of 0.00–13.14 (ave = 1.96), 0.00–3.21 (ave = 0.67), and 0.00–3.72 (ave = 0.30), respectively (Table S2 and Table 2). This suggests that the water salinity in FC is higher than that in the LCG-1 and LCG-2. In Fig. 10a, the relationship between $\delta^{13}\text{C}_{\text{EOM}}$ and β -Carotane/ $n\text{-C}_{\text{max}}$ in mudstone samples from FC and LCG Fm shows that the range of $\delta^{13}\text{C}_{\text{EOM}}$ changes gradually narrowed with the increase of β -carotane/ $n\text{-C}_{\text{max}}$ ratio. This demonstrates that during the depositional period of the LCG Fm, there were great variations in the salinity, which resulted in changes in algal types. With the increase in salinity and stabilization of sedimentary conditions in FC Fm, the type of algae tended to stabilize.

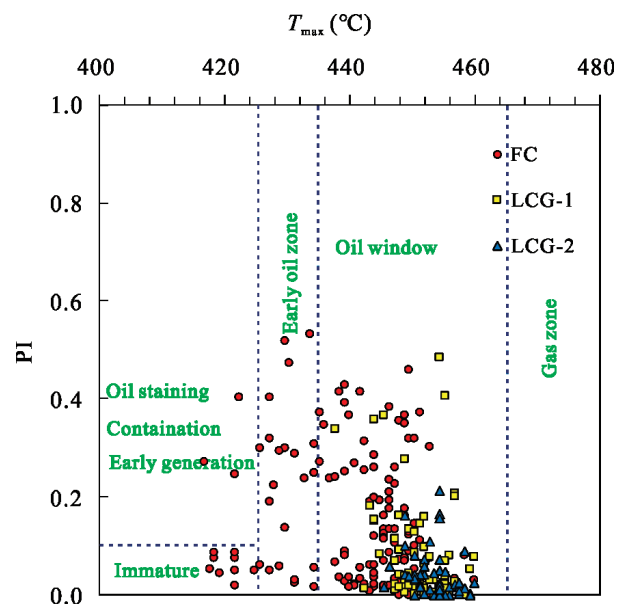


Figure 7. PI versus T_{max} diagram based on rock pyrolysis of whole rock (after Peters and Cassa, 1994).

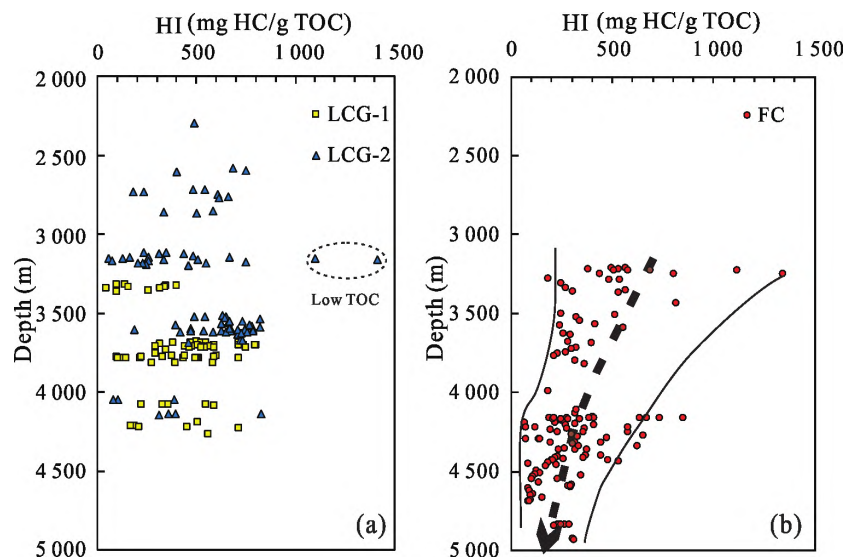


Figure 8. HI versus depth of the LCG (a) and FC (b) Fms shale in Mahu and Jimusaer sags, Junggar Basin, NW China.

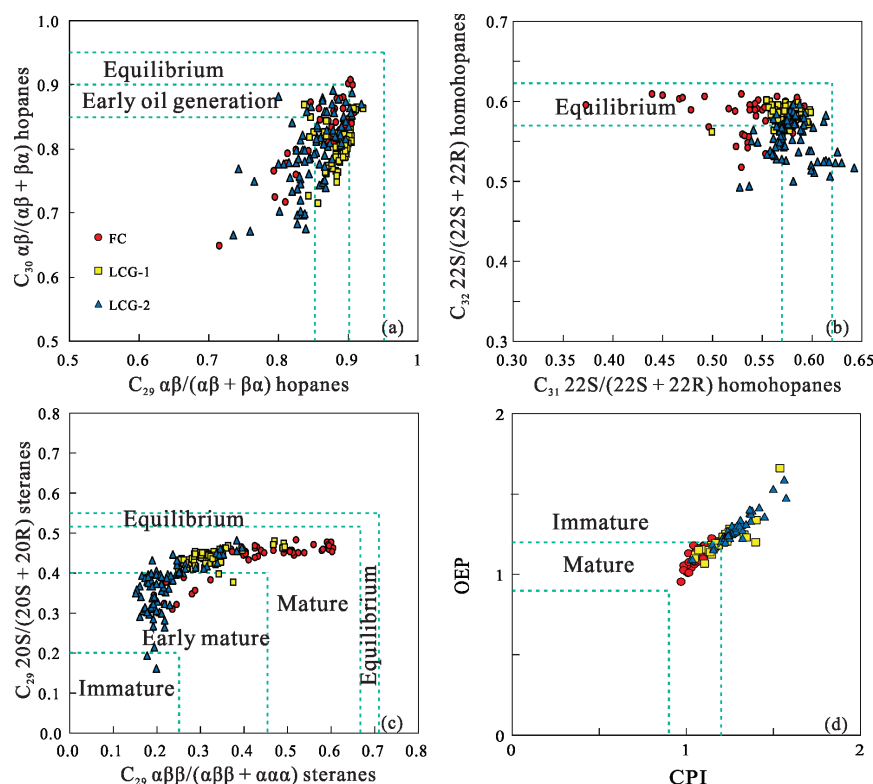


Figure 9. Cross-plots of (a) $C_{30} \alpha\beta/(\alpha\beta + \beta\alpha)$ hopanes versus $C_{29} \alpha\beta/(\alpha\beta + \beta\alpha)$ hopanes (after George et al., 2001); (b) $C_{31} 22S/(22S + 22R)$ homohopanes versus $C_{32} 22S/(22S + 22R)$ homohopanes (after Seifert and Moldowan, 1986); (c) $C_{29} \alpha\alpha\alpha 20S/(20S + 20R)$ sterane versus $C_{29} \alpha\beta\beta/(\alpha\beta\beta + \alpha\alpha\alpha)$ sterane (after Seifert and Moldowan, 1986); (d) CPI versus OEP (after Scanlan and Smith, 1970) of the FC and LCG Fm shale in Mahu and Jimusaer sag, Junggar Basin, NW China.

The distribution patterns of the C_{27} , C_{28} , and C_{29} regular steranes are closely related to the sources of different algae. Most shale samples have distribution patterns of $\alpha\alpha\alpha 20R C_{27} < C_{28} < C_{29}$ sterane (Fig. 4, Table S2). As seen in Fig. 10b, the ratios of the C_{27}/C_{29} regular steranes and those of the C_{28}/C_{29} regular steranes of LCG-2 varied greatly, while the ratios of samples from LCG-1 and FC Fm changed little and tended to be stable. This indicates that, with the increase in salinity, the algal diversity was simplified and stabilized in the source rock samples from LCG to FC Fm. This is consistent with the results from organic petrological observation.

Hopanes are thought to originate from precursors in bacterial membranes (Peters et al., 2005). The hopanes/steranes ratios were considered to represent the relative contribution of bacteria and eukaryotes to organic matter (Summons et al., 2006). The gammacerane content is often used to analyze water salinity in the sedimentary environment and the practically used gammacerane index (gammacerane/ C_{30} hopane ratio) increases with the increase in water salinity (Wang, 1990; Moldowan et al., 1986). As shown in Fig. 10c, LCG Fm shales were mainly deposited in the depositional environment of anoxic-dysoxic normal-to-higher salinity with a weakly stratified water column while the FC Fm shales were mainly deposited in a depositional environment with higher salinity and a stratified water column. The high abundance of hopanes and high ratios of hopanes/steranes in LCG Fm indicated that strong bacterial activity occurs during the depositional and diagenetic processes (Fig. 10c and Table S2). However, the ratios of hopanes/steranes in the FC Fm were lower, indicating that the bacterial

contribution was weakened in a depositional environment with higher salinity. The $i-C_{21}/n-C_{19}$ ratios can be used to represent the relative contribution of halophilic archaea (Brassell et al., 1981). In Fig. 10d, the contribution of halophilic archaea to the FC Fm was greater than that of the LCG Fm. This agrees with the fact the methanophilus is more developed in the depocenter than in the sedimentary margin of the Mahu sag by Xia et al. (2021).

The $Ph/n-C_{18}$ versus $Pr/n-C_{17}$ plot is often used to determine the organic matter input and depositional conditions of source rocks (Shanmugam, 1985; Connan and Cassou, 1980). Figure 11a indicates that the LCG Fm shales were deposited in the transitional to reducing environment with algal and mixed organic matter, while the FC Fm shales were deposited in a diametrically different environment that was anoxic and dominated by algal input. High C_{19} , C_{20} , and C_{21} tricyclic terpanes are related to organic matter of terrestrial origin (Ozcelik and Altunsi, 2005; Peters et al., 2005), and high C_{23} tricyclic terpane is associated with high marine matter contributions (Ourisson et al., 1982) or highly reducing marine carbonate settings (Waples and Machihara, 1991). The FC Fm has high C_{22}/C_{21} and low C_{20}/C_{23} TT (tricyclic terpane) values (Fig. 11b, Table S2, Table 2), while the LCG Fm sediments have low C_{22}/C_{21} and high C_{20}/C_{23} TT values, indicating high contribution of terrestrial organic matter in the LCG Fm and lower salinity of sedimentary water than the FC Fm (Fig. 11b). This conclusion is also supported by the β -carotane/ $n-C_{max}$ and gammacerane/ C_{30} hopane ratios. Pr/Ph ratios less than 1 indicate anoxic depositional environments, whereas a Pr/Ph greater than 3 indicates a

suboxic to oxic depositional environment (Philp, 1994; Powell and McKirdy, 1973). The increase in phytane (Ph) content indicated an increase in the salinity of sedimentary water and the input of planktonic algae (Mello et al., 1988; Shanmugam, 1985; Connan and Cassou, 1980). In Fig. 11c, it can be observed that the LCG Fm was mainly formed in an anoxic to dysoxic/suboxic lacustrine depositional environment while the FC Fm was formed in an environment with stronger reducing conditions, in which the water medium was characterized by higher salinity and greater input of planktonic algal organic matter. In addition, the ratios of Pr/Ph and Ph/C₁₈ varied widely from FC to LCG Fm, indicating that the sedimentary conditions changed greatly while the biological sources changed gradually during the depositional periods from the FC Fm to LCG Fm.

4.3 Organic Matter Enrichment and Hydrocarbon Potential under the Control of Different Water Salinities

Predecessors have conducted substantial research on the enrichment conditions of organic matter in the study area, especially the influence of hydrothermal and tephra (Cao et al., 2020). However, changes in these external conditions will largely affect the nature of sedimentary water body. Therefore, this study is mainly aimed at the influence of water salinity, stratification properties and terrestrial source supply on the formation of source rocks.

The average TOC contents in the shales were 1.06 wt.% for FC Fm, 4.06 wt.% for LCG-1 Member, and 5.67 wt.% for LCG-2 Member (Table 1). Although FC Fm source rocks are currently in a higher evolution stage, the generation and expulsion of hydrocarbons by organic matter will result in lower

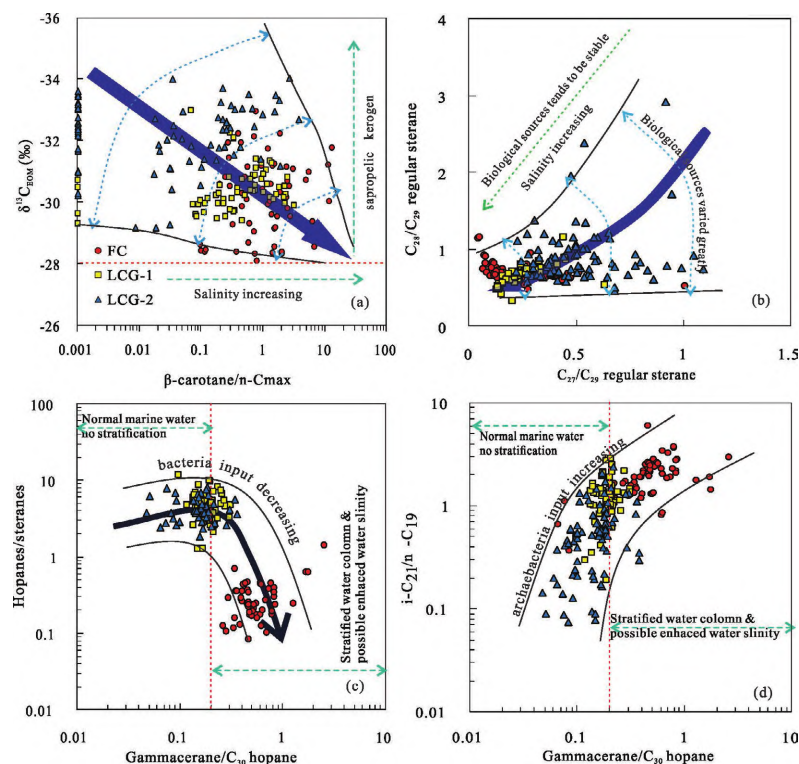


Figure 10. Cross-plots of (a) $\delta^{13}C_{EOM}$ versus β -carotane/ n -C_{max}; (b) C_{28}/C_{29} regular sterane versus C_{27}/C_{29} regular sterane; (c) hopanes/steranes versus gammacerane/ C_{30} hopane; (d) i -C₂₁/ n -C₁₉ versus gammacerane/ C_{30} hopane of the FC and LCG Fm shale in Mahu and Jimusaer sag, Junggar Basin, NW China.

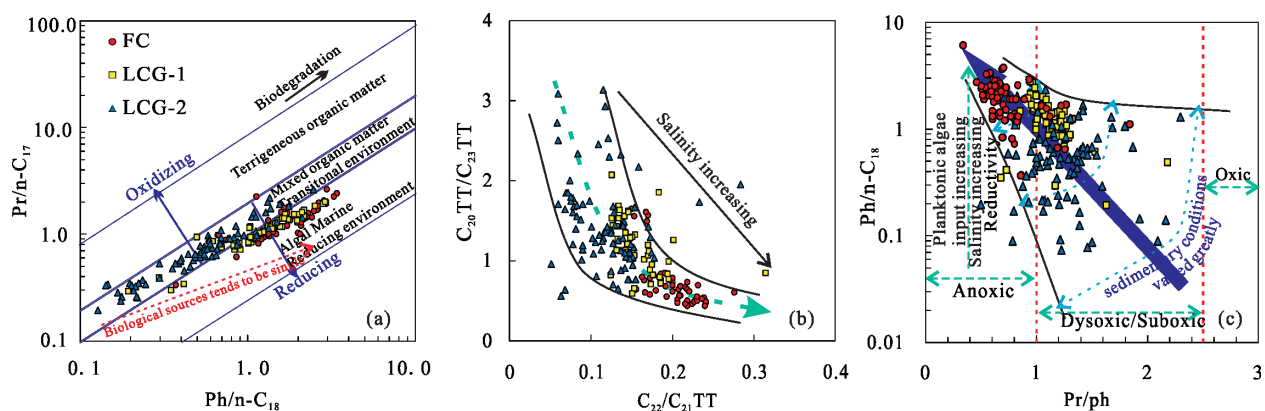


Figure 11. Crossplot of (a) Pr/ n -C₁₇ versus Ph/ n -C₁₈ (after Connan and Cassou, 1980); (b) C_{20}/C_{23} TT versus C_{22}/C_{21} TT; (c) Pr/Ph versus Ph/ n -C₁₈ of the FC and LCG Fm shale in Mahu and Jimusaer sag, Junggar Basin, NW China.

TOC values today. However, the comparison of TOC values from the two formations indicate that there are great differences in the averages and maxima of TOC values in the two formations, generally the organic carbon content of the FC Fm is generally lower than that in the LCG Fm. According to organic petrological observation, the organic matter was extremely enriched in the LCG Fm mudstone and the plane porosity of individual organic matter particle in the LCG Fm was much higher than that of the source rocks in the FC Fm (Figs. 5 and 6). This further illustrated that the organic matter in the LCG Fm is more enriched. As seen in Fig. 12a, as the salinity of sedimentary water increased, the TOC content in the LCG-1 Member and FC Fm gradually decreased. And the degree of organic matter enrichment was relatively decreased (Fig. 12a). It can be seen from Fig. 12b that as the increase of salinity, the $(S_1 + S_2)/\text{TOC}$ parameters of source rocks were gradually concentrated in high-value areas and the middle-lower $(S_1 + S_2)/\text{TOC}$ ratios of some source rocks in the FC Fm is mainly related to the high degree of evolution. During the depositional period of the LCG Fm, Strong input of freshwater and higher plants, which provides a large amount of nutrients and the deposition conditions vary greatly, resulting the propagation and diversification of algae (halophilic algae and halophobic algae) which favors the enrichment of organic matter (Figs. 13a and 13b). This will also lead to the strong heterogeneity of organic matter in the source rocks of the LCG Fm (Fig. 6 and Fig. 12a). In FC formation sedimentation process, it is characterized by weak input of freshwater and higher plants in arid climate and high salinity of sedimentary water body, the halophilic algae are well developed (Fig. 13c). Therefore, the organic matter diversities of the FC Fm will be restricted, but the degree of organic matter enrichment was relatively more stable (Fig. 12a). Moreover, the source rocks in the FC Fm, with low supply of terrestrial organic matter and primary source dominated aquatic algae, has a higher primary hydrocarbon-generating potential than LCG Fm (Fig. 2 and Fig. 12b). Under different salinity deposition conditions, the maximum $(S_1 + S_2)/\text{TOC}$ values in the source rock

samples of the LCG Fm and the FC Fm were not much different (Fig. 12b), indicating that both the two types of algae (algae A and algae B in Figs. 5–6) organic matter have high conversion rate to generate hydrocarbons. Therefore, the organic matter accumulation in the FC, LCG-1, and LCG-2 shales was controlled by different contributions of varying parental materials and sedimentary environments.

High quality source rocks are developed in different lacustrine basins in China. Such as Shahejie Formation, Qinsankou Formation etc. A lot of work has been done on the study of organic matter enrichment (Yin et al., 2020; Zhao et al., 2020; Ding et al., 2019). In this study, the organic matter enrichment was discussed from the relationship between environmental changes of source rock deposition and the development of biodiversity. Aquatic organisms in sedimentary water may have different ecological characteristics, which may lead to the development and enrichment of different organisms in different environments. Further clarifying the sources of different organic organisms in sedimentary rocks and their corresponding development environments is helpful to further deepen the mechanism of organic matter enrichment.

5 CONCLUSION

A series of experiments including TOC analysis, Rock-Eval, stable carbon isotope analyses, and biomarker analyses of the FC Fm and LCG Fm were conducted to decipher geochemical parameters such as thermal maturity, biological sources, sedimentary environments, organic matter accumulation, and hydrocarbon potential. The result show that the LCG Fm shales are generally good-to-excellent source rocks and have been still in the early-to-medium maturity stage. The FC Fm has fair-to-good source rocks with Type I–II₁ kerogen favorable for oil generation and in the thermally mature stage.

During the deposition of FC Fm, LCG-1 Member, and LCG-2 Member, the environment for the formation of source rocks changed first by a gradual decrease in salinity to redox to dysoxic/suboxic depositional conditions then to a gradually

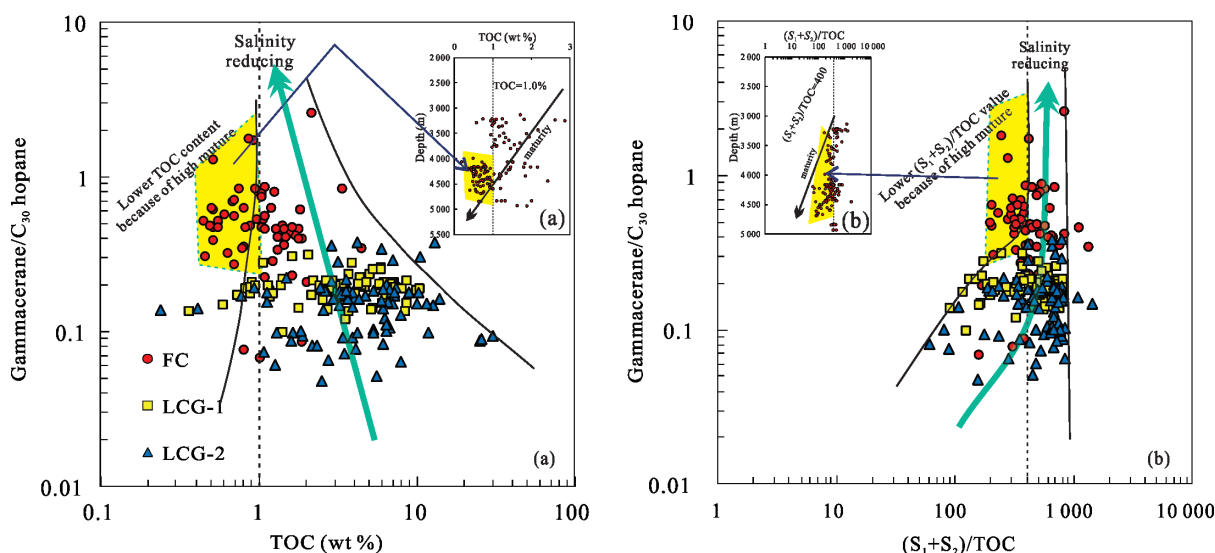


Figure 12. The cross diagrams of TOC versus gammacerane/ C_{30} hopane (a) and $(S_1 + S_2)/\text{TOC} \times 100$ versus gammacerane/ C_{30} hopane ratios (b) of the FC and LCG Fm shale in Mahu and Jimusaer sag, Junggar Basin, NW China.

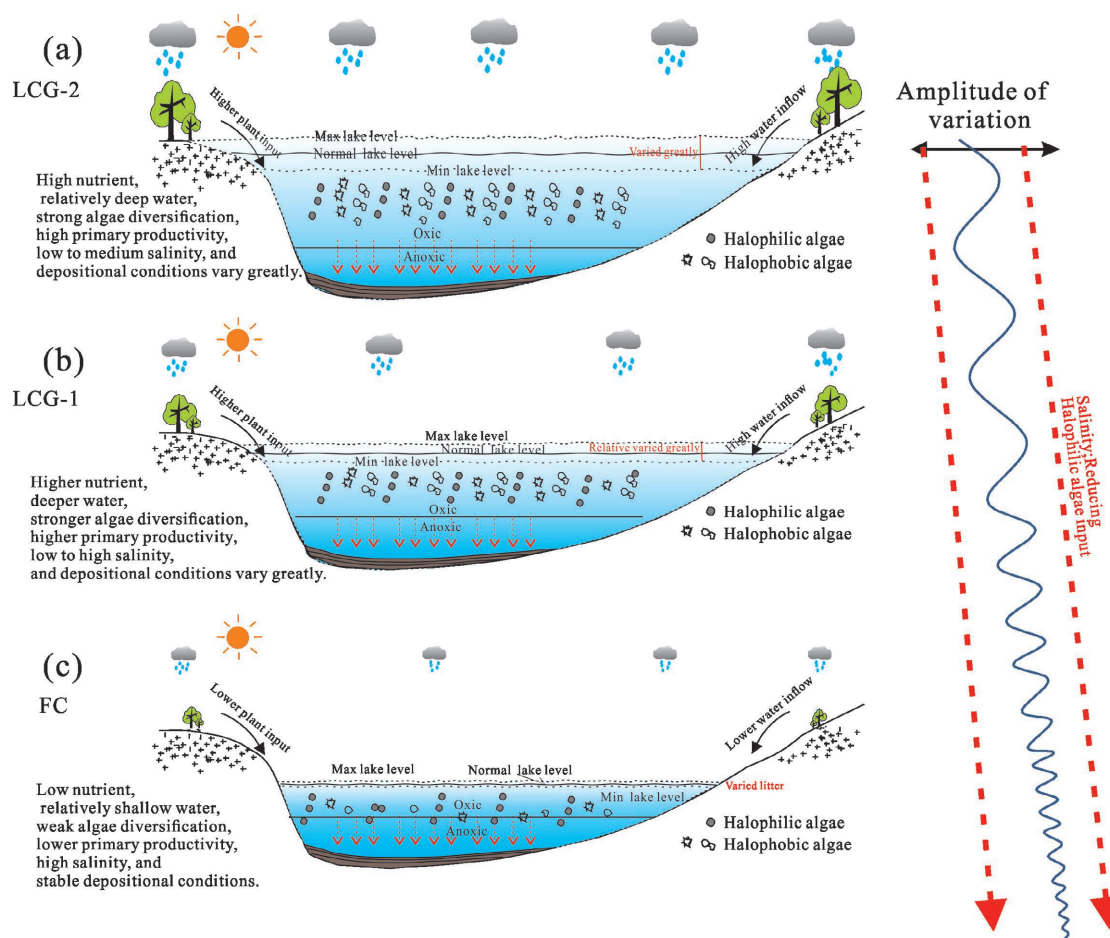


Figure 13. Scheme for the enrichment of organic matter in LCG-2 (a), LCG-1(b) and FC Fm (c). (a) Strong input of freshwater and higher plants, which provides a large amount of nutrients and the deposition conditions vary greatly, resulting the propagation and diversification of algae which favors the enrichment of organic matter. (b) There is also strong freshwater and higher plants input, but slightly lower than (a). The degree of organic matter enrichment is also slightly lower than (a). (c) it is characterized by weak input of freshwater and higher plants in arid climate and high salinity of sedimentary water body. The depositional conditions are stable, the halophilic algae is well developed in the water body; therefore the organic matter accumulation is restricted.

weakened water stratification, and finally resulted in a deterioration of the stability of depositional conditions.

The biomarker composition indicate that the mudstone of the FC Fm mainly formed in a high salinity and strong reduction sedimentary environment. The biogenic precursor was mainly planktonic algae and salt-tolerant archaea. With low salinity and frequent changes in the sedimentary conditions, the development of algal diversity, terrestrial organism and the contribution of bacteria increased in the LCG Fm.

The organic matter in the FC Fm mudstone was monotonously sourced that the degree of organic matter enrichment is weaker than that in the LCG Fm. But the FC Fm mudstone is homogenous and have higher primary hydrocarbon-generating potential.

ACKNOWLEDGMENTS

We would like to thank Xinjiang Oilfield Company for allowing the publication of this manuscript and for providing us for part of the analyzed geochemistry data on the shales and stratigraphic framework. The final publication is available at Springer via <https://doi.org/10.1007/s12583-021-1566-0>.

Electronic Supplementary Materials: Supplementary materials (Tables S1–S2) are available in the online version of this article at <https://doi.org/10.1007/s12583-021-1566-0>.

Conflict of Interest

The authors declare that they have no conflict of interest.

REFERENCES CITED

- Borjigen, T., Qin, J. Z., Fu, X. D., et al., 2014. Marine Hydrocarbon Source Rocks of the Upper Permian Longtan Formation and Their Contribution to Gas Accumulation in the Northeastern Sichuan Basin, Southwest China. *Marine and Petroleum Geology*, 57: 160–172. <https://doi.org/10.1016/j.marpetgeo.2014.05.005>
- Brassell, S. C., Wardrop, A. M. K., Thomson, I. D., et al., 1981. Specific Acyclic Isoprenoids as Biological Markers of Methanogenic Bacteria in Marine Sediments. *Nature*, 290(5808): 693–696. <https://doi.org/10.1038/290693a0>
- Bray, E. E., Evans, E. D., 1961. Distribution of *n*-Paraffins as a Clue to Recognition of Source Beds. *Geochimica et Cosmochimica Acta*, 22(1): 2–15. [https://doi.org/10.1016/0016-7037\(61\)90069-2](https://doi.org/10.1016/0016-7037(61)90069-2)
- Cao, J., Xia, L. W., Wang, T. T., et al., 2020. An Alkaline Lake in the Late Paleozoic Ice Age (LPIA): A Review and New Insights into

- Paleoenvironment and Petroleum Geology. *Earth-Science Reviews*, 202: 103091. <https://doi.org/10.1016/j.earscirev.2020.103091>
- Che, C. B., Zhu, J., Li, F. B., et al., 2010. The Status Quo and Developing Trend of Global Hydrocarbon Resources. *Natural Gas Industry*, 30(1): 1–4, 133 (in Chinese with English Abstract)
- Chen, J. P., Deng, C. P., Song, F. Q., et al., 2007. Mathematical Calculating Model Using Biomarkers to Quantitatively Determine Relative Source Proportion of Mixed Oils. *Geochimica*, 36(2): 205–214. <https://doi.org/10.19700/j.0379-1726.2007.02.011> (in Chinese with English Abstract)
- Cheng, K. M., 1994. Oil and Gas Generation of Tuha Basin. Petroleum Industry Press, Beijing (in Chinese)
- Connan, J., Cassou, A. M., 1980. Properties of Gases and Petroleum Liquids Derived from Terrestrial Kerogen at Various Maturation Levels. *Geochimica et Cosmochimica Acta*, 44(1): 1–23. [https://doi.org/10.1016/0016-7037\(80\)90173-8](https://doi.org/10.1016/0016-7037(80)90173-8)
- Ding, X. J., Qu, J. X., Imin, A., et al., 2019. Organic Matter Origin and Accumulation in Tuffaceous Shale of the Lower Permian Lucaogou Formation, Jimsar Sag. *Journal of Petroleum Science and Engineering*, 179: 696–706. <https://doi.org/10.1016/j.petrol.2019.05.004>
- Duan, Y., Peng, D. H., Zhang, X. B., et al., 2003. Main Controlling Factors and Genetic Types of Carbon Isotopic Compositions for Crude Oils from the Qaidam Basin, China. *Acta Sedimentologica Sinica*, 21(2): 355–359 (in Chinese with English Abstract)
- Gao, G., Liu, X. Y., Wang, Y. H., et al., 2013. Characteristics and Resource Potential of the Oil Shale of Chang 7 Layer in Longdong Area, Ordos Basin. *Earth Science Frontiers*, 20(2): 140–146 (in Chinese with English Abstract)
- Gao, G., Yang, S. R., Ren, J. L., et al., 2018. Geochemistry and Depositional Conditions of the Carbonate-Bearing Lacustrine Source Rocks: A Case Study from the Early Permian Fengcheng Formation of Well FN₁ in the Northwestern Junggar Basin. *Journal of Petroleum Science and Engineering*, 162: 407–418. <https://doi.org/10.1016/j.petrol.2017.12.065>
- Gao, G., Zhang, W. W., Xiang, B. L., et al., 2016. Geochemistry Characteristics and Hydrocarbon-Generating Potential of Lacustrine Source Rock in Lucaogou Formation of the Jimusaer Sag, Junggar Basin. *Journal of Petroleum Science and Engineering*, 145: 168–182. <https://doi.org/10.1016/j.petrol.2016.03.023>
- George, S. C., Ruble, T. E., Dutkiewicz, A., et al., 2001. Assessing the Maturity of Oil Trapped in Fluid Inclusions Using Molecular Geochemistry Data and Visually-Determined Fluorescence Colours. *Applied Geochemistry*, 16(4): 451–473. [https://doi.org/10.1016/S0883-2927\(00\)00051-2](https://doi.org/10.1016/S0883-2927(00)00051-2)
- Ghanizadeh, A., Clarkson, C. R., Aquino, S., et al., 2015. Petrophysical and Geomechanical Characteristics of Canadian Tight Oil and Liquid-Rich Gas Reservoirs: I. Pore Network and Permeability Characterization. *Fuel*, 153: 664–681. <https://doi.org/10.1016/j.fuel.2015.03.020>
- Guo, J. Y., Li, Z. M., 2009. Study of Gas Source and Characteristics of Carboniferous Hydrocarbon Source Rock in the Junggar Basin. *Petroleum Geology & Experiment*, 31(3): 275–281 (in Chinese with English Abstract)
- Hackley, P. C., Fishman, N., Wu, T., et al., 2016. Organic Petrology and Geochemistry of Mudrocks from the Lacustrine Lucaogou Formation, Santanghu Basin, Northwest China: Application to Lake Basin Evolution. *International Journal of Coal Geology*, 168: 20–34. <https://doi.org/10.1016/j.coal.2016.05.011>
- Hall, P. B., Douglas, A. G., 1981. The Distribution of Cyclic Alkanes in Two Lacustrine Deposits. Hjaray, M., Albrecht, C., Cornford, C., et al., Advances in Organic Geochemistry. John Wiley & Sons, Chichester. 576–587
- Huang, D. F., Li, J. C., Gu, X. Z., 1984. Evolution and Hydrocarbon-Generating Mechanism of Terrigenous Organic Matter. Petroleum Industry Press, Beijing
- Jarvie, D. M., 2010. Unconventional Oil Petroleum Systems: Shales and Shale Hybrids. AAPG Conference and Exhibition, September 12–15, 2010, Calgary, Alberta, Canada
- Jarvie, D. M., 2012. Shale Resource Systems for Oil and Gas: Part 1. Shale-Gas Resource Systems. In: Breyer, J. A., ed., Shale Reservoirs—Giant Resources for the 21st Century. AAPG Memoir, 97: 89–119. <https://doi.org/10.1306/13321446m973489>
- Jiang, Y. Q., Liu, Y. Q., Yang, Z., et al., 2015. Characteristics and Origin of Tuff-Type Tight Oil in Jimusar Depression, Junggar Basin, NW China. *Petroleum Exploration and Development*, 42(6): 741–749 (in Chinese with English Abstract)
- Jiang, Z. S., Fowler, M. G., 1986. Carotenoid-Derived Alkanes in Oils from Northwestern China. *Organic Geochemistry*, 10(4/5/6): 831–839. [https://doi.org/10.1016/S0146-6380\(86\)80020-1](https://doi.org/10.1016/S0146-6380(86)80020-1)
- Yin, J., Hao, F., Wang, Z. Q., et al., 2020. Lacustrine Conditions Control on the Distribution of Organic-Rich Source Rocks: An Instance Analysis of the Lower 1st Member of the Shahejie Formation in the Raoyang Sag, Bohai Bay Basin. *Journal of Natural Gas Science and Engineering*, 78: 103320. <https://doi.org/10.1016/j.jngse.2020.103320>
- Jin, Q., Zhu, G. Y., Wang, J., 2008. Deposition and Distribution of High-Potential Source Rocks in Saline Lacustrine Environments. *Journal of China University of Petroleum (Edition of Natural Science)*, 32(4): 19–23 (in Chinese with English Abstract)
- Kates, M., 1977. The Phytanyl Ether-Linked Polar Lipids and Isoprenoid Neutral Lipids of Extremely Halophilic Bacteria. *Progress in the Chemistry of Fats and Other Lipids*, 15(4): 301–342. [https://doi.org/10.1016/0079-6832\(77\)90011-8](https://doi.org/10.1016/0079-6832(77)90011-8)
- Kuang, J., Liu, D. G., Chen, X. F., 1999. Natural Gas Reservoir Formation and Exploration Directions in Junggar Basin. *China Petroleum Exploration*, 4: 28–32 (in Chinese with English Abstract)
- Kuang, L. C., Hu, W., Wang, X., et al., 2013. Research of the Tight Oil Reservoir in the LCG Formation in Jimusaer Sag: Analysis of Lithology and Porosity Characteristics. *Geology Journal of China University*, 19: 529–535 (in Chinese with English Abstract)
- Kuang, L. C., Tang, Y., Lei, D. W., et al., 2012. Formation Conditions and Exploration Potential of Tight Oil in the Permian Saline Lacustrine Dolomitic Rock, Junggar Basin, NW China. *Petroleum Exploration and Development*, 39(6): 700–711. [https://doi.org/10.1016/S1876-3804\(12\)60095-0](https://doi.org/10.1016/S1876-3804(12)60095-0)
- Kuhn, P. P., di Primio, R., Hill, R., et al., 2012. Three-Dimensional Modeling Study of the Low-Permeability Petroleum System of the Bakken Formation. *AAPG Bulletin*, 96(10): 1867–1897. <https://doi.org/10.1306/03261211063>
- Li, Y., Cao, D. Y., Wu, P., et al., 2017. Variation in Maceral Composition and Gas Content with Vitrinite Reflectance in Bituminous Coal of the Eastern Ordos Basin, China. *Journal of Petroleum Science and Engineering*, 149: 114–125. <https://doi.org/10.1016/j.petrol.2016.10.018>
- Li, Y., Wang, Z. S., Gan, Q., et al., 2019a. Paleoenvironmental Conditions and Organic Matter Accumulation in Upper Paleozoic Organic-Rich Rocks in the East Margin of the Ordos Basin, China. *Fuel*, 252: 172–187. <https://doi.org/10.1016/j.fuel.2019.04.095>

- Li, Y., Wang, Z. S., Wu, P., et al., 2019b. Organic Geochemistry of Upper Paleozoic Source Rocks in the Eastern Margin of the Ordos Basin, China: Input and Hydrocarbon Generation Potential. *Journal of Petroleum Science and Engineering*, 181: 106202. <https://doi.org/10.1016/j.petrol.2019.106202>
- Liang, S. J., Huang, Z. L., Liu, B., et al., 2012. Formation Mechanism and Enrichment Conditions of Lucaogou Formation Shale Oil from Malang Sag, Santanghu Basin. *Acta Petrolei Sinica*, 33(4): 588–594 (in Chinese with English Abstract)
- Liu, B., Sun, J. H., Zhang, Y. Q., et al., 2021. Reservoir Space and Enrichment Model of Shale Oil in the First Member of Cretaceous Qingshankou Formation in the Changling Sag, Southern Songliao Basin, NE China. *Petroleum Exploration and Development*, 48(3): 608–624. [https://doi.org/10.1016/S1876-3804\(21\)60049-6](https://doi.org/10.1016/S1876-3804(21)60049-6)
- Liu, Z. J., Liu, R., 2005. Oil Shale Resource State and Evaluation System. *Earth Science Frontiers*, 12(3): 315–323 (in Chinese with English Abstract)
- Liu, B., Bechtel, A., Sachsenhofer, R. F., et al., 2017. Depositional Environment of Oil Shale within the Second Member of Permian Lucaogou Formation in the Santanghu Basin, Northwest China. *International Journal of Coal Geology*, 175: 10–25. <https://doi.org/10.1016/j.coal.2017.03.011>
- Liu, B., Bechtel, A., Gross, D., et al., 2018. Middle Permian Environmental Changes and Shale Oil Potential Evidenced by High-Resolution Organic Petrology, Geochemistry and Mineral Composition of the Sediments in the Santanghu Basin, Northwest China. *International Journal of Coal Geology*, 185: 119–137. <https://doi.org/10.1016/j.coal.2017.11.015>
- Liu, C. M., Cheng, X. S., Zhao, Z. Y., et al., 2006. Oil Source and Reservoir-Forming Analysis of East Slope in Jumusa'er Sag, Junggar Basin. *Natural Gas Exploration and Development*, 29(3): 5–7, 69 (in Chinese with English Abstract)
- Lu, X. C., Kong, Y. H., Chang, J., et al., 2012. Characteristics and Main Controlling Factors of Sand-Gravel Stone Reservoir of Permian Fengcheng Formation in Kebai Area, Northwest Junggar Basin. *Natural Gas Geoscience*, 3: 474–481 (in Chinese with English Abstract)
- Luo, Q. Y., George, S. C., Xu, Y. H., et al., 2016. Organic Geochemical Characteristics of the Mesoproterozoic Hongshuizhuang Formation from Northern China: Implications for Thermal Maturity and Biological Sources. *Organic Geochemistry*, 99: 23–37. <https://doi.org/10.1016/j.orggeochem.2016.05.004>
- Luo, Q. Y., Gong, L., Qu, Y. S., et al., 2018. The Tight Oil Potential of the Lucaogou Formation from the Southern Junggar Basin, China. *Fuel*, 234: 858–871. <https://doi.org/10.1016/j.fuel.2018.07.002>
- Mello, M. R., Telnaes, N., Gaglianone, P. C., et al., 1988. Organic Geochemical Characterisation of Depositional Palaeoenvironments of Source Rocks and Oils in Brazilian Marginal Basins. *Organic Geochemistry*, 13(1/2/3): 31–45. [https://doi.org/10.1016/0146-6380\(88\)90023-X](https://doi.org/10.1016/0146-6380(88)90023-X)
- Moldowan, J. M., Sundaraman, P., Schoell, M., 1986. Sensitivity of Biomarker Properties to Depositional Environment and/or Source Input in the Lower Toarcian of SW-Germany. *Organic Geochemistry*, 10(4/5/6): 915–926. [https://doi.org/10.1016/S0146-6380\(86\)80029-8](https://doi.org/10.1016/S0146-6380(86)80029-8)
- Mukhopadhyay, P. K., Wade, J. A., Kruger, M. A., 1995. Organic Facies and Maturation of Jurassic/Cretaceous Rocks, and Possible Oil-Source Rock Correlation Based on Pyrolysis of Asphaltenes, Scotian Basin, Canada. *Organic Geochemistry*, 22(1): 85–104. [https://doi.org/10.1016/0146-6380\(95\)90010-1](https://doi.org/10.1016/0146-6380(95)90010-1)
- Nie, H. K., Zhang, P. X., Bian, R. K., et al., 2016. Oil Accumulation Characteristics of China Continental Shale. *Earth Science Frontiers*, 23(2): 55–62. (in Chinese with English Abstract)
- Ouriou, G., Albrecht, P., Rohmer, M., 1982. Predictive Microbial Biochemistry—From Molecular Fossils to Prokaryotic Membranes. *Trends in Biochemical Sciences*, 7(7): 236–239. [https://doi.org/10.1016/0968-0004\(82\)90028-7](https://doi.org/10.1016/0968-0004(82)90028-7)
- Ozcelik, O., Altunsoy, M., 2005. Organic Geochemical Characteristics of Miocene Bituminous Units in the Beypazari Basin, Central Anatolia, Turkey. *Arabian Journal for Science and Engineering*, 30(2): 181–194.
- Peters, K. E., Cassa, M. R., 1994. Applied Source Rock Geochemistry. In: Magoon, L. B., Dow, W. G., eds., *The Petroleum System—From Source to Trap*. American Association of Petroleum Geologists, Tulsa. 93–120 <https://doi.org/10.1306/m60585c5>
- Peters, K. E., Walters, C. C., Moldowan, J. M., 2005. *The Biomarker Guide: 2nd Edition. Biomarkers and Isotopes in Petroleum Systems and Earth History (II)*. University Press, Cambridge
- Philp, R. P., 1994. Geochemical Characteristics of Oils Derived Predominantly from Terrigenous Source Materials. *Geological Society, London, Special Publications*, 77(1): 71–91. <https://doi.org/10.1144/gsl.sp.1994.077.01.04>
- Powell, T. G., McKirdy, D. M., 1973. Relationship between Ratio of Pristane to Phytane, Crude Oil Composition and Geological Environment in Australia. *Nature Physical Science*, 243(124): 37–39. <https://doi.org/10.1038/physci243037a0>
- Qu, C. S., Qiu, L. W., Cao, Y. C., et al., 2017. Organic Petrology Characteristics and Occurrence of Source Rocks in Permian Lucaogou Formation, Jimsar Sag. *Journal of China University of Petroleum (Edition of Natural Science)*, 41(2): 30–38 (in Chinese with English Abstract)
- Ren J. L., Jin J., Ma W. Y., et al., 2017. Analysis of Hydrocarbon Potential of Fengcheng Saline Lacustrine Source Rock of Lower Permian in Mahu Sag, Junggar Basin. *Geological Review*, 63(S1): 51–52. <https://doi.org/10.16509/j.georeview.2017.s1.026> (in Chinese with English Abstract).
- Scalan, E. S., Smith, J. E., 1970. An Improved Measure of the Odd-Even Predominance in the Normal Alkanes of Sediment Extracts and Petroleum. *Geochimica et Cosmochimica Acta*, 34(5): 611–620. [https://doi.org/10.1016/0016-7037\(70\)90019-0](https://doi.org/10.1016/0016-7037(70)90019-0)
- Seifert, W. K., Moldowan, J. M., 1986. Use of Biological Markers in Petroleum Exploration. *Methods in Geochemistry and Geophysics*, 24: 261–290
- Shanmugam, G., 1985. Significance of Coniferous Rain Forests and Related Organic Matter in Generating Commercial Quantities of Oil, Gippsland Basin, Australia. *AAPG Bulletin*, 69: 1241–1254. <https://doi.org/10.1306/ad462bc3-16f7-11d7-8645000102c1865d>
- Shi, X., Wang, X. L., Zhang, X., et al., 2005. Distribution of Carboniferous Hydrocarbon Source Rock in Junggar Basin and Geochemical Characteristics. *China Petroleum Exploration*, 10(1): 34–39 (in Chinese with English Abstract)
- Summons, R. E., Bradley, A. S., Jahnke, L. L., et al., 2006. Steroids, Triterpenoids and Molecular Oxygen. *Philosophical Transactions of the Royal Society of London Series B, Biological Sciences*, 361(1470): 951–968. <https://doi.org/10.1098/rstb.2006.1837>
- Sun, J., 2012. Study on Litho Stratigraphic Hydrocarbon Reservoir of the Wutonggou Formation Permian in Jimusar Sag of Junggar Basin. *Journal of Southwest Petroleum University (Science & Technology)*

- Edition*), 34(5): 42–48 (in Chinese with English Abstract)
- Tissot, B. P., Welte, D. H., 1984. Petroleum Formation and Occurrence. Springer Verlag, Berlin Heidelberg, New York
- Wang, X. J., Wang, T. T., Cao, J., 2018. Basic Characteristics and Highly Efficient Hydrocarbon Generation of Alkaline-Lacustrine Source Rocks in Fengcheng Formation of Mahu Sag. *Xinjiang Petroleum Geology*, 39(1): 9–15 (in Chinese with English Abstract)
- Wang, S. J., Hu, S. B., Wang, J. Y., 2000. The Characteristics of Heat Flow and Geothermal Field in Junggar Basin. *Chinese Journal of Geophysics*, 43(6): 816–824. <https://doi.org/10.1002/cjg2.98>
- Wang, T., 1990. Biomarker Geochemical Study. China University of Geosciences Publishing House, Beijing (in Chinese with English Abstract)
- Waples, D. W., 1985. Geochemistry in Petroleum Exploration. Human Resources and Develop. Co., Boston. 232
- Waples, D. W., Machihara, T., 1991. Biomarkers for Geologists, a Practical Guide to the Application of Steranes and Triterpanes in Petroleum Geology. American Association of Petroleum Geologists Methods in Exploration Series 9, Tulsa
- Wu, X. L., Gao, B., Ye, X., et al., 2013. Shale Oil Accumulation Conditions and Exploration Potential of Faulted Basins in the East of China. *Oil & Gas Geology*, 34(4): 455–462 (in Chinese with English Abstract)
- Xia, L. W., Cao, J., Lee, C., et al., 2021. A New Constraint on the Antiquity of Ancient Haloalkaliphilic Green Algae that Flourished in a Ca. 300 Ma Paleozoic Lake. *Geobiology*, 19(2): 147–161. <https://doi.org/10.1111/gbi.12423>
- Zhang, C. J., He, D. F., Wu, X. Z., et al., 2006. Formation and Evolution of Multicycle Superimposed Basins in Junggar Basin. *China Petroleum Exploration*, 11(1): 47–58 (in Chinese with English Abstract)
- Zhang, J., Liu, L., Huang, Y., et al., 2003. Sedimentary Characteristics of Middle–Upper Permian in Jimusaer Sag of Junggar Basin. *Xinjiang Geology*, 21(4): 412–414 (in Chinese with English Abstract)
- Zhang, Y. Q., Zhang, N. F., 2006. Oil/Gas Enrichment of Large Superimposed Basin in Junggar Basin. *China Petroleum Exploration*, 11(1): 59–64 (in Chinese with English Abstract)
- Zhao, Z. B., Littke, R., Zieger, L., et al., 2020. Depositional Environment, Thermal Maturity and Shale Oil Potential of the Cretaceous Qingshankou Formation in the Eastern Changling Sag, Songliao Basin, China: an Integrated Organic and Inorganic Geochemistry Approach. *International Journal of Coal Geology*, 232: 103621. <https://doi.org/10.1016/j.coal.2020.103621>
- Zhu, G. Y., Jin, Q., Zhang, S. W., et al., 2004. Salt Lacustrine-Saline Lacustrine Sedimentary Combination and Petroleum Accumulation in the Bonan Sag. *Acta Mineralogica Sinica*, 1: 25–30 (in Chinese with English Abstract)
- Zou, C. N., Yang, Z., Cui, J. W., et al., 2013. Formation Mechanism, Geological Characteristics and Development Strategy of Nonmarine Shale Oil in China. *Petroleum Exploration and Development*, 40(1): 14–26 (in Chinese with English Abstract)
- Zou, C. N., Tao S. Z., Hou L. H., et al., 2011. Unconventional Oil and Gas Geology. Geological Publishing House, Beijing. 128–151